Mutual Coupling Between Meteorological Parameters and Secondary Microseisms

Karel Holub[1, *], Pavel Kalenda[2], and Jana Rušajová[1]

[1] *Institute of Geonics AS CR,v.v.i., Ostrava, Czech Republic*
[2] *Institute of Rock Structure and Mechanics AS CR, v.v.i., Praha, Czech Republic*

ABSTRACT

The basic scientific question of this study was: do other mechanisms exist for excitation of secondary microseisms aside from the widely accepted mechanism by non-linear interactions of respective ocean waves. Here we use continuous broadband data from secondary microseisms recorded at the Ostrava-Krásné Pole, Czech Republic (OKC) seismic station to create a massive seismological database. Except for seismological data, various meteorological features and their mutual relations were analysed: temperature, the so called "shifted" temperature, air density, changes of atmospheric pressure, and synoptic situations. These analyses prove that maximum amplitudes of microseisms were observed during winter, while minimum amplitudes occured in summer months. The annual variations of microseisms amplitudes could not be explained by annual variations of storm activity above the North Atlantic. In addition, current analyses also aim at quantitative and quantitative evaluation of synoptic situations for triggering individual microseismic anomalies. Some of the meteorological features, namely the distribution of low pressures above northern Europe and high-pressure areas in Central Europe make it easy to explain most of the microseismic extremes. Here we pay special attention to the influence of large earthquakes, which usually induce slow deformation waves. We conclude that at least three mechanisms of microseism generation are possible: (1) the function of atmospheric pressure at sea level in the North Atlantic, (2) the effects of spreading of thermoelastic waves in the rock mass and (3) deformation waves induced by large earthquakes.

Key words: Secondary microseisms, Meteorological elements, Statistics

Citation: Holub, K., P. Kalenda, and J. Rušajová, 2013: Mutual coupling between meteorological parameters and secondary microseisms. Terr. Atmos. Ocean. Sci., 24, 933-949, doi: 10.3319/TAO.2013.07.04.01(T)

1. INTRODUCTION

It is widely accepted that microseisms are ubiquitous seismic signals generated by ocean waves (Webb 2007), especially during the winter (Zátopek 1964, 1975). Basically, two groups of microseisms, primary and secondary microseisms, are considered. Both types of microseisms have different time spans, though the limits of the spans of a certain measure vary. According to Cessaro (1994), Bromirski (2001) and Kurrle and Widmer-Schnidrig (2006), there exist primary microseisms with a predominant period within the span $T \approx 10 - 25$ s and smaller amplitude (Koper et al. 2010). These microseisms are generated through the shoaling of ocean waves. However, there are also secondary microseisms with periods $T \approx 4 - 10$ s, which have higher

spectral amplitudes than primary microseisms. Figure 1 represents compressed data of these microseisms, which usually form more or less intensive "knobs". The large amplitude is generally explained by the non-linear interactions of opposing ocean waves, as proposed by Longuet-Higgins (1950), and expanded by Tanimoto (2007a) and Webb (2007). The new theory anticipates that secondary microseisms are more likely to be generated in shallow water near the coast, as observed by many authors (Haubrich and McCamy 1969; Bromirski and Duennebier 2002; Rhie and Romanowicz 2006; Tanimoto 2007b; Gerstoft and Tanimoto 2007).

Data from the OKC seismic station (Czech Republic) ($\varphi = 49.8375°N$; $\lambda = 18.1472°E$) was used for the analysis of meteorological and secondary microseisms interactions. Maximum particle velocities (nm s^{-1}) were measured daily at night, between 23:00 and 01:00 UTC, to be disturbed as

---

* *Corresponding author*
  E-mail: holub@ugn.cas.cz
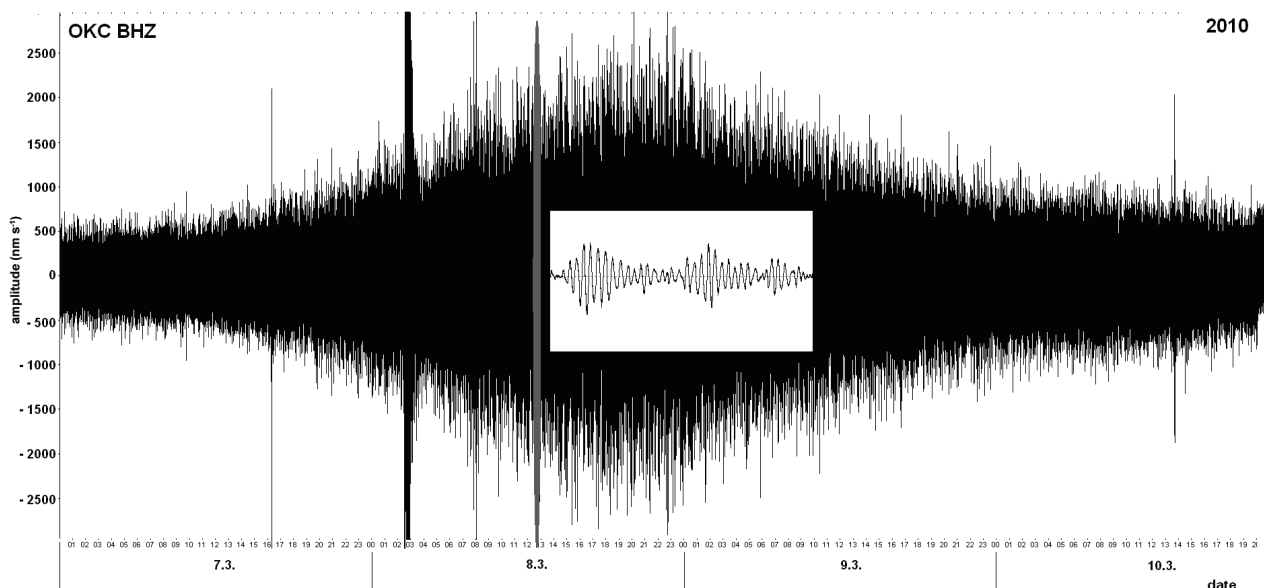
Fig. 1. Sample of compressed data of the secondary microseisms (the vertical component). The width of the gray strip in the middle of "knob" represents the time interval of short-term data (in detail with reduced amplitude).

little as possible by anthropogenic noise, and were subsequently converted to displacement amplitudes (nm). Observations used in this paper cover the time interval from January 1, 2007 to December 31, 2011. On the other hand, data concerning temperature, air density, atmospheric pressure, humidity and entalpy was obtained from the Chlumec nad Cidlinou (Czech Republic) meteorological station (φ = 50.15422°N; λ = 15.84623°E), (Chlumec 2012) for the period from January 1, 2009 to December 31, 2011. The meteorological data was obtained from the Holešov station (φ = 49.31°N; λ = 17.56°E) (Freemeteo 2007 - 2013, Weatheronline 1999 - 2013) for the period from January 1, 2007 to December 31, 2011.

All stadard meteorological parameters were analysed in the same time span and with same time step (1 day) during a year 2012. The exception was only atmospheric pressure data, where we used planar interpretations of air pressure variations for the (geopotential) level of 500 hPa, were made by Wetterzentrale (1995 - 2013). Only three meteorological parameters (air pressure data, air density, temperature) are mentioned here, because the other as humidity and enthalpy seem to be linearly correlated with the other. We analysed the meteorological parameters especially from the meteorological stations, which are not far from the OKC seismic station in comparison with the diameter of Europe and North Atlantic Ocean. The air pressure variations were analysed from the whole area between the eastern coast of North America and Ural Mountains and between North Africa and the Spitzbergen Islands (based on Wetterzentrale 1995 - 2013).

The scientific goal of this study was to specify some likely new sources of secondary microseisms, which were revealed during the detailed analysis of our experimen-

tal measurements. According to our measurement of microseisms (Holub et al. 2008, 2009) and massif deformations (Kalenda and Neumann 2010; Kalenda et al. 2009), we deduced that there are at least three other mechanisms capable of microseism generation in addition to the widely accepted mechanism of generation by ocean waves. The first mechanism can be connected with atmospheric pressure variations; the second is associated with thermoelastic waves in rock mass (Hvoždara and Brimich 1988; Brimich 2006); and, third the relationship is associated with large earthquakes (Kalenda et al. 2011, 2013). All of the proposed mechanisms are coupled with stress/pressure variations during the year and not with the water shoaling.

2. ANALYSIS OF THE INTERACTION BETWEEN METEOROLOGICAL CONDITIONS AND SECONDARY MICROSEISMS

It is generally well known that microseisms are characterized by regular annual drift, which is analogous to the drift of temperature as shown in Fig. 2. During the summer months, microseisms are low, while in the winter they usually reach maximum amplitudes. Several decades ago, this annual drift was assigned to the annual drift of windstorms in northern seas as reported, for example, by Darbyshire (1990). Let us analyse, therefore, relations between meteorological parameters, e.g., air pressure, temperature, density, humidity, and displacement amplitudes of secondary microseisms, in order to specify the reason for and the way of triggering of anomalous increases in microseisms amplitudes.

Based on calculations of all combinations of meteorological parameters versus amplitudes of microseisms, it

Diurnal maximal amplitude of microseisms and average temperature in Holešov
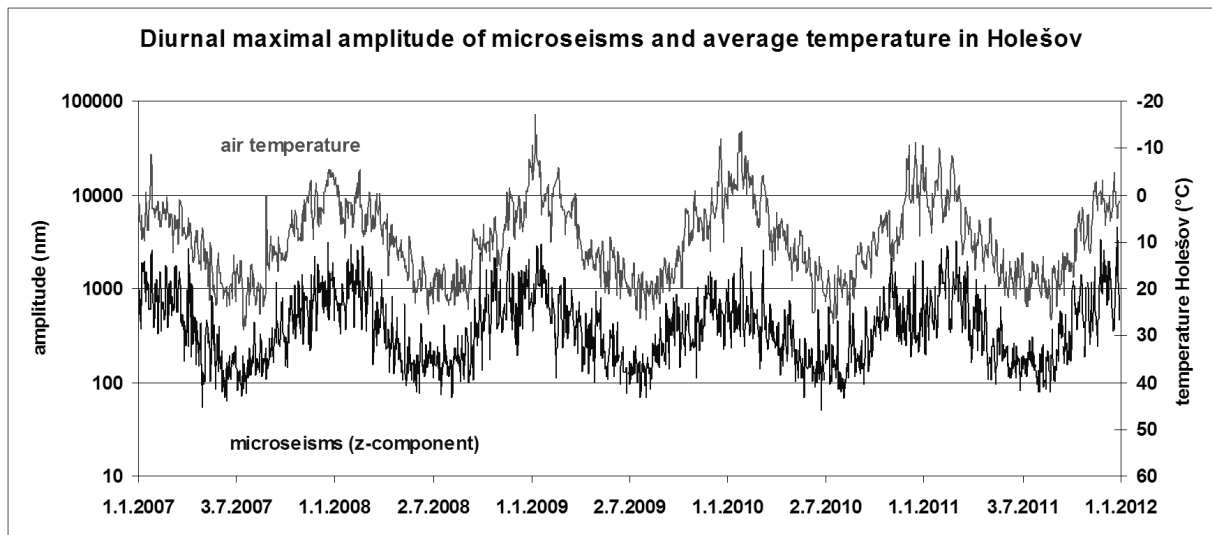
Fig. 2. Annual drift of microseisms and temperature in 2007 - 2011, obsereved at the OKC seismic station and the Holešov meteorological observatory.

was documented that the highest values of the correlation coefficient of R ~ 0.5 was found for temperature, air density and humidity versus that of microseisms (see Table 1). While the trend for temperature was negative, the correlation trend was valid for air density and humidity was positive. This information can probably be explained by the fact that all parameters, i.e., temperature, air density and humidity are mutually physically dependent each other, owing to expansibility of air. Therefore, their correlation coefficients correspond to value R = -0.97 resp. 0.92 (see Table 1).

Table 1 also includes two special parameters, namely the "shifted" temperature and the value of displacement amplitudes of microseisms expressed in the logarithmic scale. The "shifted" temperature expresses the temperature, which was on the surface 5 - 6 months ago due to delay in the spreading of thermoelastic waves as explained by Hvoždara et al. (1988). Considering that microseism amplitudes demonstrably do not present any linear response to external effects as documented in Table 1 and Fig. 3, then the correlation coefficient for the amplitudes of microseisms is lower than the correlation coefficient of amplitudes displayed in the logarithmic scale. Hereafter, under microseisms (or their residuals) only their expression in the logarithmic scale will be considered.

The annual drift of microseisms amplitudes, displayed on a logarithmic scale, can be approximated in at least two ways. First, it can be anticipated that it is a direct consequence of the drift of temperature (see Fig. 2); second, there could be a delay between surface temperature and microseisms for a couple of months. However, the first case is not physically well founded, because the penetration of heat into the depths is steady, and heat reaches a depth of approximatly 10 m in three months (Mareš et al. 1990). This thermal

wave causes the expansion of rocks beneath the weathered and loosened zone. Physically, it is reasonable to consider the phase delay of surface temperatures, taking into account the temperatures inside the unweathered rocks. Therefore, temperatures shifted back roughly 5 - 6 months, can be correlated with microseisms expressed in logarithmic scale.

It was generally stated that all physically well-founded correlations of meteorological parameters, i.e., shifted temperature, air density and relative humidity with microseisms have a lower correlation coefficient, than both of the primitive functions (saw-shaped function and cosine) with basic annual drift. We stated, after various attempts, that microseisms have an annual drift, which is explained mainly by annual variations of meteorological conditions, especially wind speed over the sea (Bromirski et al. 2005), sea wave height (in 2nd power are proportional with microseism amplitude) (Essen et al. 2003; Stehly et al. 2006), air pressure variations (Peters 2005), and coastal and sea ice conditions (Grob et al. 2011). However, this annual drift could be explained by other influences, which have an annual period, such as temperature variations, differences of air pressure or temperature between various parts of the continent, etc.

3. THE IMPACT OF METEOROLOGICAL ELEMENTS ON THE LEVEL OF SECONDARY MICROSEISMS

When we solve the problem of the influence of meteorological parameters on microseism excitation, all differences between meteorological conditions in the winter and summer of 2007 and 2008 were analysed as the first step. The meteorological situations were subtracted from the synoptical maps (Wetterzentrale 1995 - 2013). We show the daily

Table 1. Correlation coefficients between individual meteorological parameters at the station Chlumec nad Cidlinou and microseisms.

R	microseisms (nm)	air pressure (hPa)	air density (kg m^{-3})	temperature (°C)	shifted temperature* (°C)	log (microseisms) (nm)
microseisms	x	0.12923	0.50863	-0.49315	0.44733	x
air pressure	0.12923	x	0.22472	0.02000	-0.15843	0.09747
air density	0.50863	0.22472	x	**-0.96938**	0.66925	0.63679
temperature	-0.49315	0.02000	**-0.96938**	x	x	-0.63600
shifted temperature*	0.44733	-0.15843	0.66925	x	x	0.61944
log (microseisms)	x	0.09747	0.63679	-0.63600	0.61944	x
specific humidity (%)				**0.9181**		0.62346
saw-shaped function						0.70767
cosine function						0.75333

Note: (*) Shifted temperature means that the temperature is shifted 6 months in advance owing to slow penetration of temperature into depths; such temperature variations are proportional to the annual thermoelastic waves, which are generated by them.

(a)

(b)
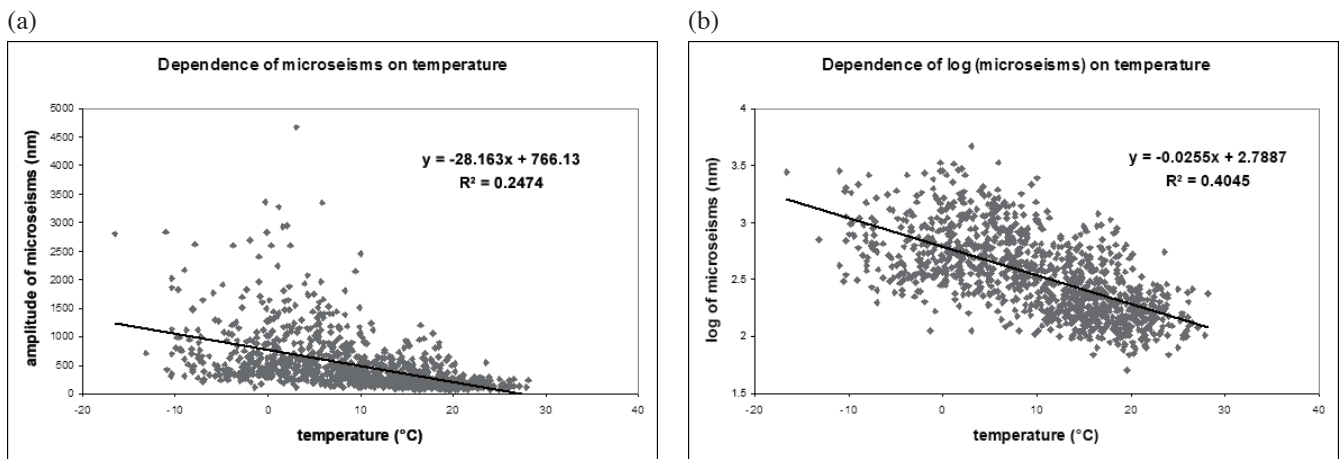
Fig. 3. Dependences: (a) displacement amplitudes versus temperature and (b) log (displacement amplitudes) versus temperature at Chlumec nad Cidlinou (Central Bohemia).

positions of pressure highs and lows with corresponding values in the raster 4 × 4 squares in Fig. 4. The sample of 100 common days with the highest and lowest amplitudes of microseisms during 2007 - 2008 were chosen for determining those months when the maxima of microseisms was observed (see Fig. 5). Both distributions have been strictly divided into winter (highest microseisms) and summer seasons (minimal microseisms). For a preliminary test of seasonal differention (winter versus summer), the two years (2007 - 2008) of observations were applied. The amplitudes of microseisms in 2009 - 2011 show generally the same behavior as seen in Fig. 2. As characteristic meteorological conditions in winter and summer, the typical periods from November 15 to March 15, and from April 15 to August 30, were selected. Two datasets were extracted from the experimental material, i.e., the meteorological conditions, which

correspond to the 100 highest and 100 lowest amplitudes of microseisms, were analysed. Then the number of pressure highs/lows anomalies was summarized, according to their area, denoted as A1 through D4 (see Tables 2a and b).

When the differences between numbers of pressure highs and lows, i.e., values in Table 2a minus Table 2b, are calculated, these numbers indicate how the number of pressure highs increased/decreased in winter versus summer for specific areas A1 - D4 (see Fig. 6). Figure 6 shows that the maximum pressure highs increase in the areas B3 and C3, and decrease in areas B2, C1 and C2 in winter, compared with summer. These annual variations of air pressure highs are commonly influenced by the seasonal temperature and wind speed variations above the sea (2 maxima in summer and in winter), and above continents (1 maximum in winter) (Arctowski 1914). The air-pressure field is much more pronounced
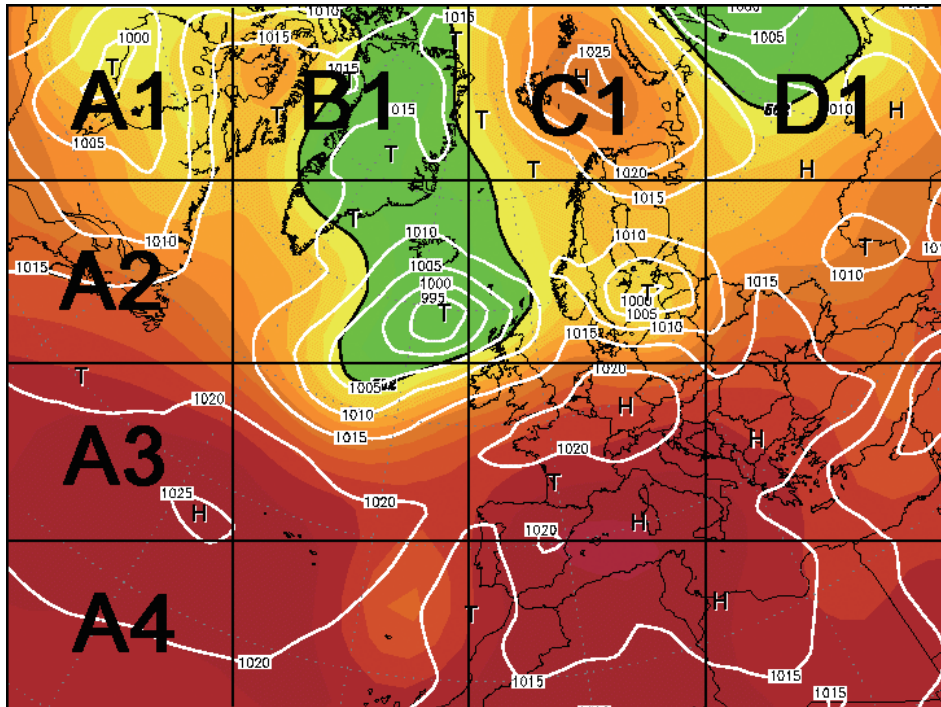
Fig. 4. The scheme of division of the map into 4 × 4 subareas A1 - D4; for example, high pressure areas A3 (1025 hPA), C1 (1025 hPa) and low B2 (995 hPa).
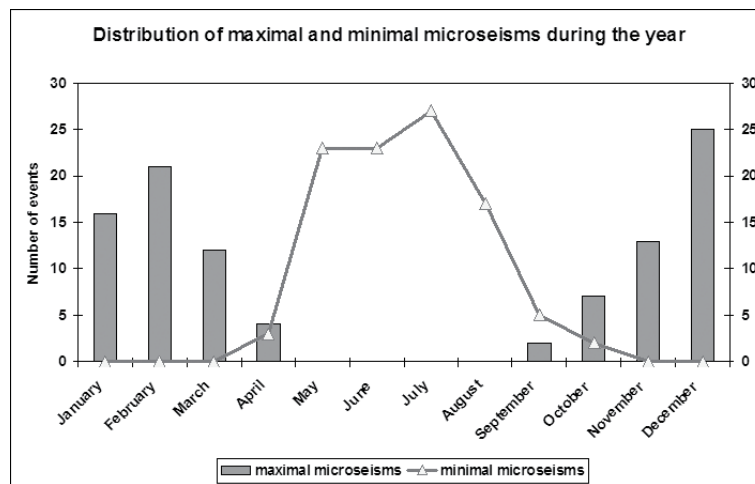
Fig. 5. The distribution of the maximal and minimal amplitudes of microseisms from 2007 - 2008. The first 100 days are used for the analysis (with maximal amplitude) and last 100 days (with minimal amplitude of microseisms).

Table 2. The differences of: (a) pressure high and (b) pressure low between winter (maximal microseisms) and summer (minimal microseisms); (c) pressure high and (d) pressure low between maximal and minimal microseisms in summer; (e) pressure high and (f) pressure low between maximal and minimal microseisms in winter. (a) Pressure height (winter-summer). (b) Low (winter-summer). (c) Pressure height (summer). (d) Low (summer). (e) Pressure height (winter). (f) Low (winter).

(a)

A	B	C	D
0	4	-2	2
0	-2	-8	3
-2	17	31	8
0	0	1	3

(b)

A	B	C	D
2	-1	30	-7
4	21	31	3
1	1	2	-1
0	0	0	0

(c)

A	B	C	D
0	-2	5	11
2	-2	-4	13
11	5	0	-2
1	-1	1	0

Table 2. (Continued)

(d)

A	B	C	D
-1	-3	**7**	**-10**
0	**10**	**12**	-1
0	**7**	**5**	-1
0	0	0	0

(e)

A	B	C	D
0	3	2	-4
0	-1	4	**-9**
-3	**14**	2	-1
0	-3	-4	2

(f)

A	B	C	D
0	2	**17**	**0**
-4	2	**8**	-5
0	**-3**	-4	0
0	0	0	0
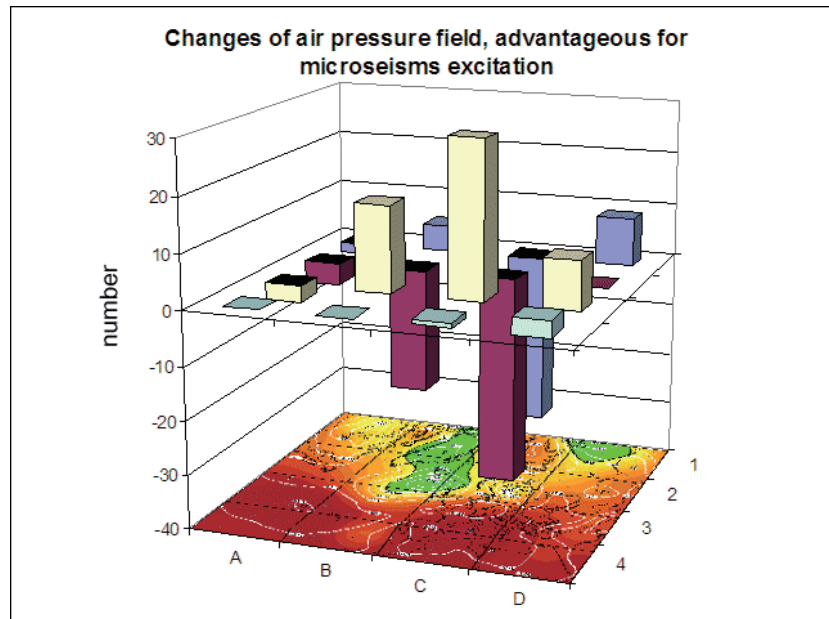
Fig. 6. The increase/decrease of number of air-pressure difference extremes are displayed for areas A1 through D4, in the period of maximal versus minimal values of microseism amplitudes. Colors of columns represent the latitude number (1 - 4).

in winter than in summer, owing to the higher-pressure gradient, and larger pressure formations. The maximal gradient occurs generally in northern Europe and southern Scandinavia. The other surrounding parts, i.e., Labrador area, middle Atlantic, Northern Africa and the Near East have much smaller seasonal variations, which did not prove such a pronounced annual drift of pressure formations.

In the second step of the solution, the process of data interpretation was oriented to the analysis of particular synoptic conditions in summer (see Tables 2c and d), which could trigger anomalous amplitudes of microseisms. To eliminate annual drift of amplitudes, which is generally influenced by the movement of pressure highs and lows, two datasets, mentioned before, were created. Using data for summer and winter intervals, we tried to determine the differences of synoptic situations, occurring within the periods of maximal and/or minimal amplitudes of microseisms. It was documented that amplitudes observed in the summer season, though they do not reach amplitudes observed during winter, were observed when larger numbers of pressure highs were found above the middle of the Atlantic, to the

west of the United Kingdom and above Siberia. At the same time, the number of pressure lows over the northern Atlantic and Scandinavia, as well as partly above Western and Central Europe, increased. Simultaneously, it was confirmed that a pressure boundary passes in an east-west direction. However, in the summer there is generally a shift of pressure lows to the south. On the other hand, it was confirmed that microseisms are probably triggered during winter by pressure highs over the Central Atlantic and Europe, and by pressure lows above Spitzbergen and Scandinavia. At the same time, the number of pressure lows slightly decreased over the Central Atlantic and Europe.

The third step of analysis focused on particular synoptic conditions in winter, when the increasing amplitude of microseisms is likely triggered during the period of pressure highs occurring over Spitzbergen and Scandinavia (see Tables 2e and f). However, simultaneously, the number of pressure highs over the Central Atlantic and Europe decreased slightly. The general trend of the air pressure increasing in squares B3 and C3 was confirmed again, while an air pressure decrease was observed in squares B2, C2, and mainly in C1.

Furthermore, these current analyses were also directed at quantitative and qualitative synoptic conditions for triggering individual microseismic anomalies. The processed dataset was the same as the set in the second step, but the evaluation of the "summer" and "winter" conditions for triggering microseisms, was carried out separately. Moreover, special attention was paid to squares B2, B3 and C1, C2 and C3. The construction of histograms was based upon the frequency of pressure highs and/or lows, for maximal or minimal amplitudes of microseisms. Then the conditions for studying the quantitative statistical data, with a bearing on the synoptic situations leading to triggering microseisms, were evaluated.

Figure 7 shows that, in the summer season, the general courses of both curves in squares B2 and C2 are very similar, regardless of the character of the microseisms level. Square B2 indicates, qualitavely as well as quantitavely, that a decrease of air pressure in this region causes a higher level of microseisms, whereas in square C2, the conditions for the generation of microseisms are almost the same. In contrast, in square B3, pressure highs predominate, but their frequencies do not increase considerably. On the other hand, the number of pressure lows increases slightly. However, the average value in the centre of lows decreased by about 20 hPa within the time periods of higher microseisms. Under the same microseisms level the number of lows increased, but their pressure range remained pratically unchanged. As for "summer microseisms", we can finally conclude that they are predominant, but their frequencies did not increase considerably. On the other hand, the number of pressure lows increased slightly. However, the average value in the centre of lows decreased by about 20 hPa within the time periods of higher microseisms. Under the same level of microseisms the number of lows increased, but their pressure range remained pratically unchanged. As for "summer microseisms", we can finally conclude that they are excited owing to a fall in barometric pressure in squares B2 and C2, rather than to an increase in air pressure in squares B3 and C3.

Similar analysis was performed for the "winter season", using an identical approach. Figure 8 shows that in square B2 the number of pressure highs increased negligibly from the statistical viewpoint. However, their level is practically the same within the interval of a higher and/or lower level of microseisms. Opposite to that, within the interval of intensified microseisms, the number of lows in square C2 increased significantly, but the average value in the middle of their distribution fell. As for "winter microseisms", it can be concluded that they are excited, owing to a fall in barometric pressure in squares B2 and C2, rather than the increase of air pressure in squares B3 and C3. The movement of the pressure boundary between pressure highs (in the south) and lows (in the north) is influenced, first of all, by the annual drift of pressure formations. In the winter, these formations shift more to the north, and their pressure difference rises.

In the fourth step, we analysed how invividual synoptic situations are reflected in anomalous (maximal/minimal) microseisms observed over 2007 - 2008. For all microseismic data (daily sampling), a vector of synoptic situations was added on in squares A1 through D4, while the score was calculated. The score represents the number of situations, which probably led to the excitation of microseisms. These conditions were as follows:

(1) Low pressure is above B2 and C2.
(2) High pressure is above B3 and C3.
(3) Above B2 and C2 there is no pressure high.
(4) Somewhere above squares B2, C2, C1 a pronounced low < 975 hPa exists.
(5) Somewhere above squares B3, C3 a pressure high > 1035 hPa exists.
(6) In winter, above B2 the low is deeper than 970 hPa, and C2, deeper than 980 hPa.
(7) In winter: the pressure highs above B3 and C3 exceed the limit of 1030 hPa.
(8) In summer: the lows above B2 and C2 is deeper than 990 hPa.

The approach applied here is based on the calculation of residual microseisms such that the normal level of microseisms was approximated by a goniometric function with a maximum on January 1 and a minimum on July 2. The resulting value was substracted from observed microseisms. The obtained residuals are distributed normally. Simultaneously, they show how many times the observed values were higher/less than they should be during standard meteorological expectations and/or other conditions. The graphical form of investigated dependence of microseisms residual amplitude on synopsis score in Fig. 9 shows that though the influence of meteorological conditions for triggering a microseism is obvious. The low correlation coefficient (0.186 ± 0.035) indicates that the coupling is not too strong. If only the "winter microseisms" are displayed, then the coupling is almost the same, and the synopsis score is a little higher (0.5 pts) than for both seasons. The question is, whether the amplified microseisms (residuals > 0.1), with a score less than average value for the regression straight-line (see Fig. 9), are not triggered by other sources, e.g., earthquakes (see Fig. 10).

A histogram of frequency occurrence times of potential anomalous microseisms after earthquakes (see Fig. 10) was constructed, and compared, subsequently, with an analogously constructed histogram of all microseisms with a low score (below the regression straight line). Data interpretation of this situation proved that the set of intensive microseisms probably triggered by earthquakes exceeds the dataset comprised of all times, within the interval between 4 and 7 days after strong earthquakes (see Fig. 11). Considering that the slope of corresponding regression straight line is steeper (see Fig. 12), the influence of meteorological conditions to microseisms excitation is higher than for the whole dataset. This fact gives evidence of the non-linearity
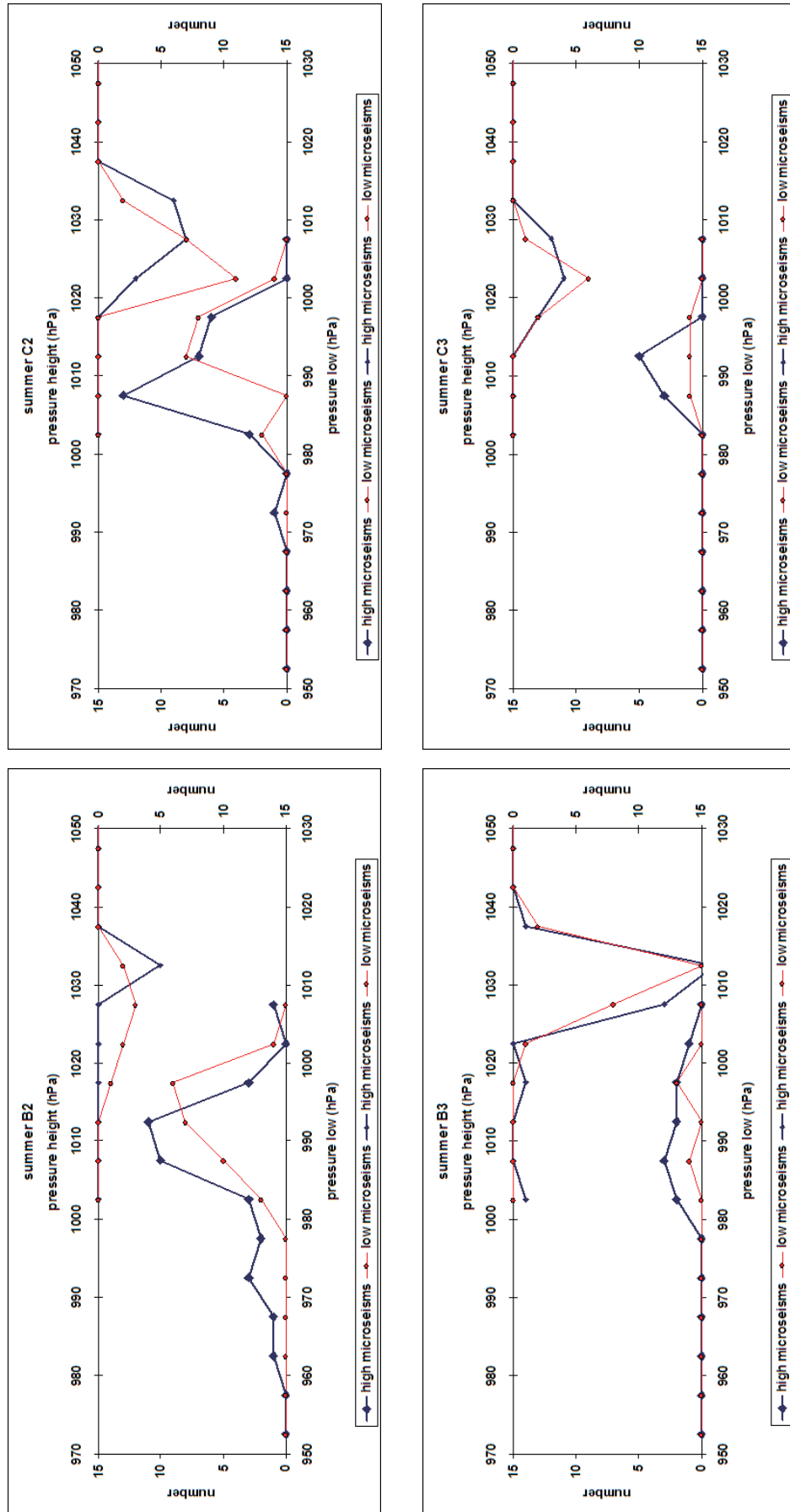
Fig. 7. The number of the pressure highs and/or lows in squares B2, B3, C2 and C3 in the summer season. The blue curve represents numbers within the period of maximal amplitudes of microseisms; the red curve corresponds to numbers within the period of minimal microseisms.
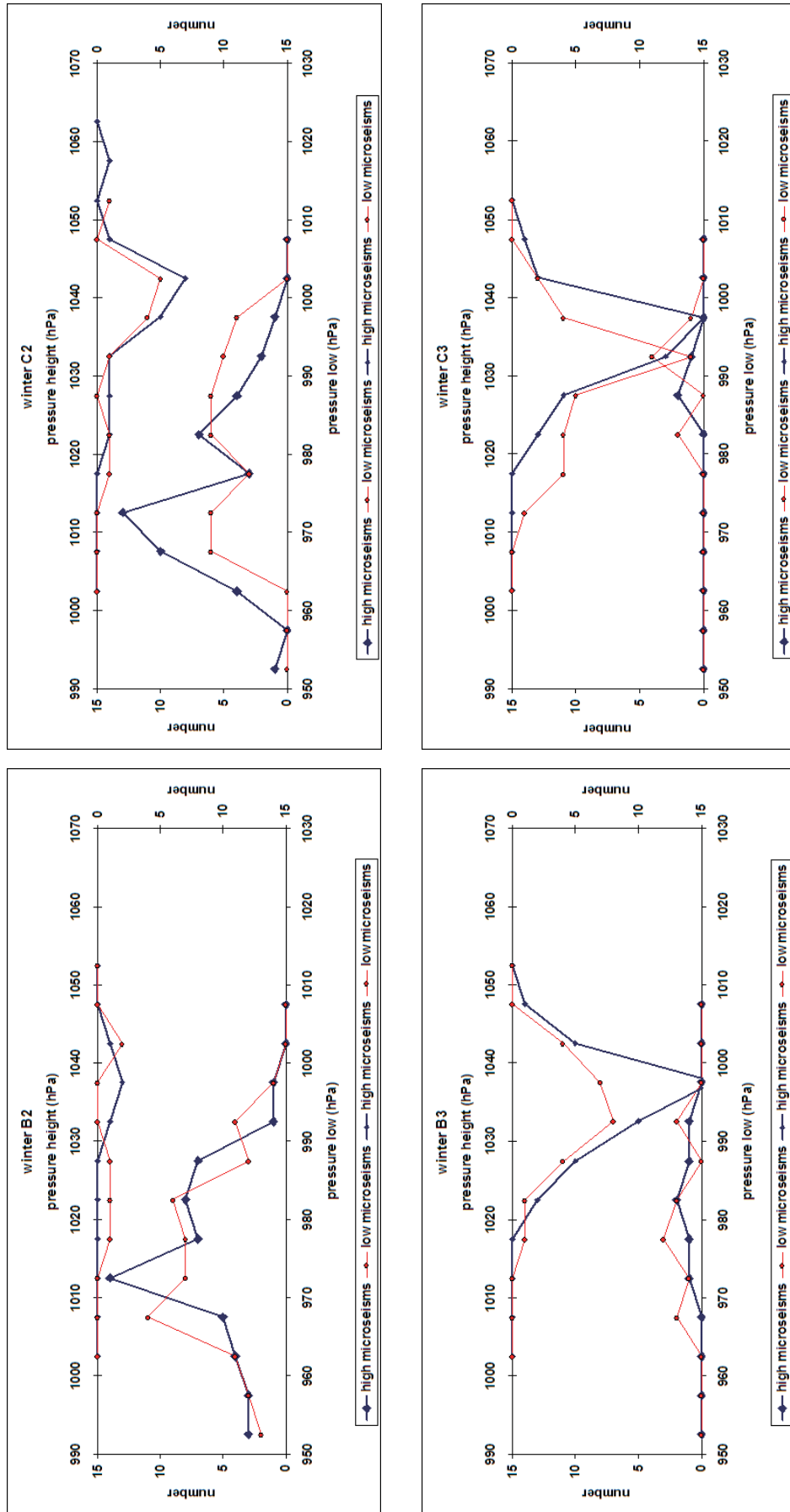
Fig. 8. The number of pressure highs in squares B2, B3, C2 and C3 within the winter season. The blue curve represents numbers in the period of maximal amplitudes of microseisms; the red curve corresponds to numbers in the period of minimal microseisms.
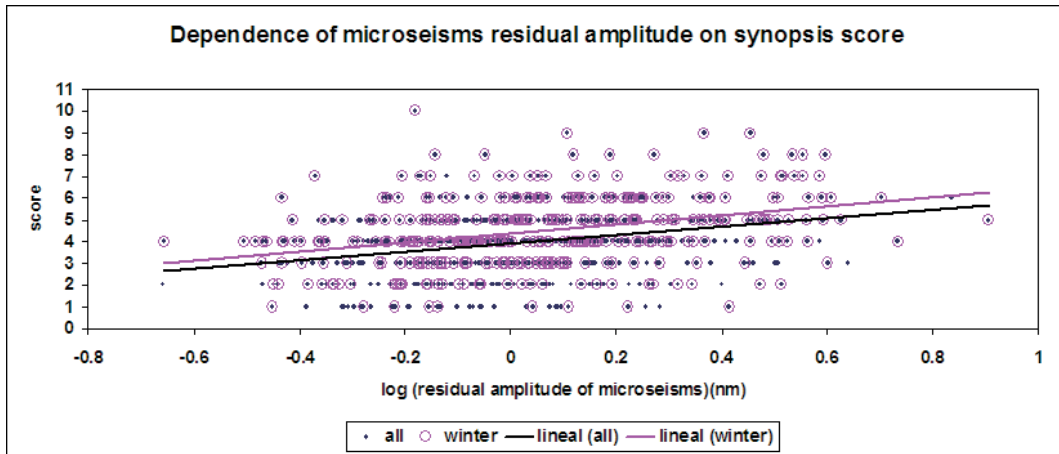
Fig. 9. Dependence of residual microseism amplitude versus synopsis score. Symbols in blue represent all data observed. Symbols in violet denote data observed during winter only.
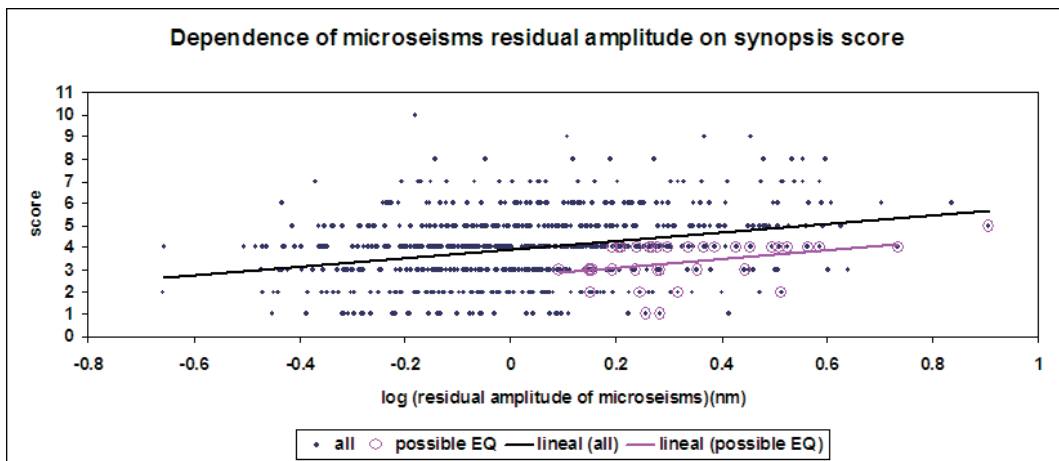
Fig. 10. Dependence of residual microseism amplitude versus synopsis score. Symbols in blue characterize all data observed. Symbols in violet represent microseisms possible influenced by earthquakes of M7+ occurring up to16 days before.
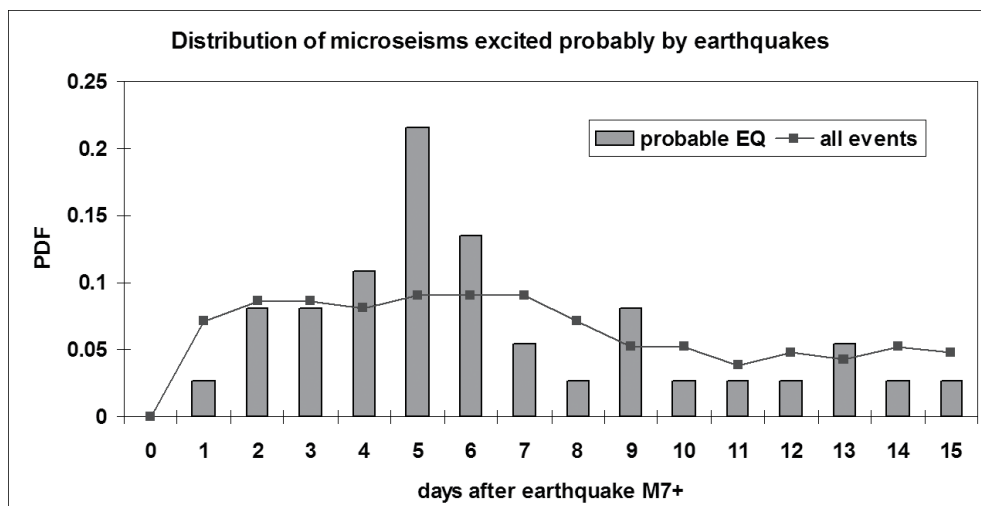
Fig. 11. Distribution of microseisms after earthquakes M7+. The bars correspond to a high level of microseism amplitudes with small scores; the curve corresponds to all microseisms with small scores.
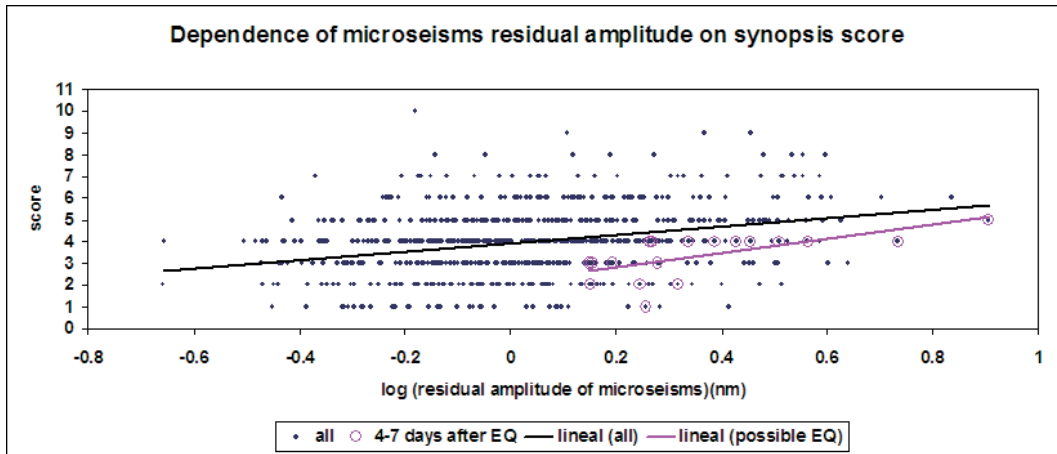
Fig. 12. Dependence of residual microseisms on synopsis scores. Symbols in violet represent microseisms possible influenced by earthquakes of M7+ occurring 4 - 7 days before.

of meteorological conditions' influence on triggering microseismic anomalies.

Similarly, if we were engaged in the study of a group of anomalously intensive residual amplitudes of microseisms > 0.4 with a high score value, then we would probably find an almost similar distribution of time series of their occurrence after strong earthquakes. Part of these intensive microseisms was excited under suitable meteorological conditions by strong earthquakes. For example, the microseisms on February 23, 2008 (microseisms = 0.7, score = 6), 3.66 days after earthquake $M_w = 7.4$ can be shown.

On the other hand, there were some cases, when favorable meteorological conditions and/or earthquakes did not excite microseisms. For instance, the microseisms on January 2, 2007 (microseisms = 0.18, score = 10), 7.48 days after earthquake $M_w = 7.1$ are evident. Then it could be pressumed that meteorological conditions and earthquakes are only triggering mechanisms. Moreover, there exists one more source, which (together with meteotrological conditions) creates the basic frame of possible microseism excitation. This mechanism could be stress variations, which has the annual period and which is generated by thermoelastic wave (Kalenda et al. 2012).

4. THE INFLUENCE OF LARGE EARTHQUAKES

The meteorological features, namely the distribution of low pressure above northern Europe and high pressure above Central Europe, enable us to explain most microseismic extremes. There remain only some peaks of microseisms without direct connection to these meteorological features. It is not possible to compensate extreme microseisms by meteorological parameters. These extreme microseisms were observed mostly from 4 to 14 days after the world's strongest earthquakes. This is documeted, for example, by the earthquakes in Chile (M = 8.8), Mentawai (M = 7.7),

and/or Tohoku (M = 9) (see Fig. 13 and Table 3).

As shown in a previous paper by Kalenda et al. (2011), the deformation waves propagate from the focal region of earthquakes with very low velocities (approx. 100 km h^{-1}), along tectonic discontinuities or boundaries (Golovachev et al. 2011). After the M > 8 earthquakes, deformation waves, travelling several times around the globe, were detected. The best example is the Chilean earthquake in 2010, when this deformation wave was detectable at observatories by means of vertical static pendulums and seismometers, three times during two months. The arrival delay of the deformation wave from the region of Indonesia was about 4 - 10 days, and from South America approximately 10 - 25 days. Most of these waves travel along the discontinuities, in the direction from east to west, probably due to the western drift of the lithosphere (Crespi et al. 2007). In contrast, the prevailing propagation of these waves after the Tohoku earthquake, in 2011, was observed across the North Pole through the northern and southern Atlantic, thence around the South Pole to the Pacific. These waves generated microseisms, especially at observatories in Greenland, Spitzbergen and the Pacific (Kalenda et al. 2011). Based on detailed analysis of seismological data, it was proven that the spectra of secondary microseisms excited by deformation waves are different from the spectra of microseisms influenced by meterological features, as represented in Fig. 14.

5. CONCLUSION

Other than the widely accepted mechanism of generation of secondary microseisms by ocean waves, we propose three other possible mechanisms that excite microseisms activities: (1) atmospheric pressure variations, (2) generation of the thermoelastic waves in rock mass and (3) deformation waves generated by large earthquakes. The main influence has the second type of mechanism, generation of the
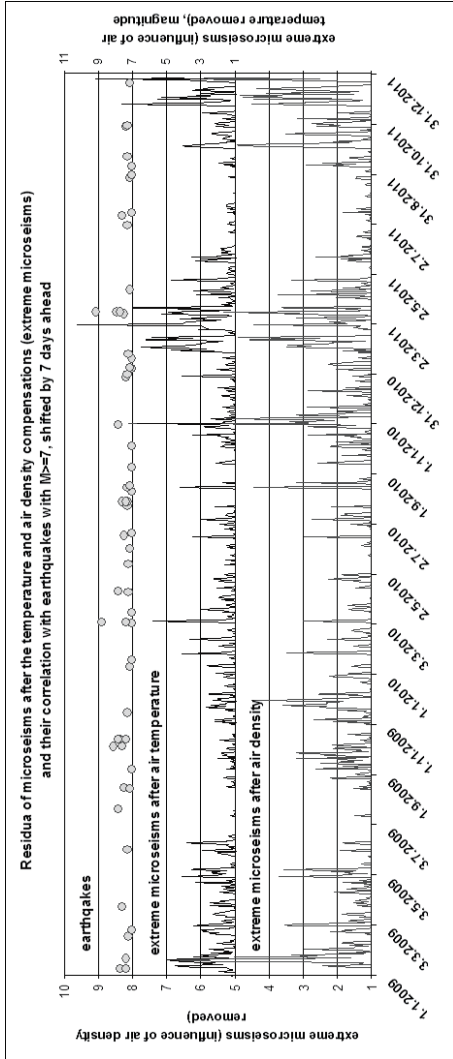
Fig. 13. Comparison of earthquakes M > 7 worldwide with non-compensated microseisms according to temperature and air density.

Table 3. Extreme amplitudes of microseisms and likely existing reasons.

date of microseism	amplitude of microseisms (nm)	synoptic feature	earthquakes	lat	lon	depth	M	days after EQ
28.1.2007	2572.84	depression above the Iceland						
23.2.2007	1775.79							
14.3.2007	1759.84	depression above N. Atlantic						
20.3.2007	1497.33	depression above Scandinavia						
6.4.2007	2717.5	depression above Scandinavia / Iceland	1.4.2007	-8.4660	157.043	24	8.1	4.1
12.4.2007	1135.85	depression above Greenland						
20.5.2007	843.43							
16.9.2007	1159.06		12.9.2007	-4.4380	101.367	34	8.5	3.5
26.11.2007	2202.18	depression above N. Atlantic	14.11.2007	-22.2470	-69.89	40	7.7	11.3
21.12.2007	3170.96	depression above N. Atlantic	9.12.2007	-25.9960	-177.514	152.5	7.8	11.7
2.2.2008	2966.29	depression above Scandinavia						
15.2.2008	2575.01	depression above German ocean						
24.2.2008	2896.82	express. depr. above Greenland + Scandi.						
11.3.2008	1525.09	depression above Iceland + Greenland						

Table 3. (Continued)

date of microseism	amplitude of microseisms (nm)	synoptic feature	earthquakes	lat	lon	depth	M	days after EQ
30.3.2008	1230.69	depression above Spitsbergen						
18.4.2008	824.41	depression above Spitsbergen						
11.5.2008	689.56							
11.6.2008	420.91							
24.7.2008	407.23							
19.9.2008	787.99	inexpressive depression above the Iceland						
28.9.2008	2405.15	inexpressive depression above the Iceland						
11.10.2008	1590.13	depression N of Greenland						
24.10.2008	1404.7	**expressive depre above Iceland + Greenland**						
26.10.2008	2115.32	**expressive depression above Iceland**						
22.11.2008	2780.28	**expressive depression above Scandinavia**						
13.1.2009	2831.43	depression above Greenland	3.1.2009	-0.4140	132.885	17	7.7	9.2
20.1.2009	2939.98	depression above the Iceland	15.1.2009	46.8570	155.154	36	7.4	4.3
4.3.2009	1322.6	**expressive depression SW of Iceland**						
2.5.2009	939.55	depression above German sea + Greenland						
11.5.2009	812.29	depression above Greenland						
3.6.2009	426.9		28.5.2009	16.7310	-86.217	19	7.3	5.6
12.6.2009	432.13		28.5.2009	16.7310	-86.217	19	7.3	14.6
11.9.2009	708.38	inexpressive depression NW of Greenland						
23.9.2009	795.65	depression above Greenland						
29.9.2009	893.73	depression above Scandinavia						
27.11.2009	1392.81	depression above Scandinavia + Greenland						
28.1.2010	2804.73	depression W of Scandinavia	12.1.2010	18.4430	-72.571	13	7	15.1
9.3.2010	2595.38	depression above Spitsbergen	27.2.2010	-37.7730	-75.048	35	7.4	9.7
28.4.2010	756.86		4.4.2010	32.2163	-115.301	10	7.2	23.1
19.6.2010	596.86		12.6.2010	7.8810	91.936	35	7.5	6.2
9.7.2010	635.64	air pressure drop in Chlumec						
25.7.2010	452.29		18.7.2010	-5.9310	150.59	35	7.3	6.4

Table 3. (Continued)

date of microseism	amplitude of microseisms (nm)	synoptic feature	earthquakes	lat	lon	depth	M	days after EQ
17.8.2010	899.32		10.8.2010	-17.5410	168.069	25	7.3	6.8
23.8.2010	553.5		12.8.2010	-1.2660	-77.306	206.7	7.1	10.5
20.10.2010	1069.8	depression between Sweeden and Greenland						
2.11.2010	2456.25	depression N of Spitsbergen	25.10.2010	-3.4870	100.082	20.1	7.8	7.4
9.11.2010	1508.19	**expressive depression above Spitsbergen**						
17.12.2010	1859.04	depression between Greenland and Scandi.						
31.12.2010	2023.57	depression above German sea and Greenland	21.12.2010	26.9010	143.698	14	7.4	9.3
4.2.2011	2697.28	**expressive depr. above Iceland + Greenland**						
13.2.2011	2840.14	complicated depression above Iceland + Finland						
3.3.2011	3278.5	depression above N. Atlantic + Greenland						
9.3.2011	1713.93	**expressive depr. above Iceland + Greenland**						
18.3.2011	1502.46	**depression above Greenland**	9.3.2011	38.4350	142.842	32	7.5	8.9
23.3.2011	1958.53	depression above German sea	11.3.2011	38.2970	142.373	29	9.1	11.8
9.4.2011	1237.5	depression NW of Greenland						
16.4.2011	871.32	depression SW of Greenland	7.4.2011	38.2760	141.588	42	7.1	8.4
26.4.2011	1107.1	depression W of Greenland						
24.5.2011	644.32							
6.10.2011	1192.12	inexpressive depression above the Iceland						
11.10.2011	700.55	complicated depr. above Iceland + German sea						
21.10.2011	1408.78	depression above Greenland						
8.11.2011	1165.7	depression above the Iceland						
26.11.2011	3367.58	**expressive depression above Iceland**						
2.12.2011	2601.89	**expressive depression NE of Iceland**						
4.12.2011	2064.06	depression E of Iceland						
9.12.2011	1918.8	complicated depr. above Iceland + German sea						
15.12.2011	1645.94	depression E of Iceland						
26.12.2011	4664.69	**expressive depression NE of Iceland**	14.12.2011	-7.5610	146.804	140.9	7.1	11.8
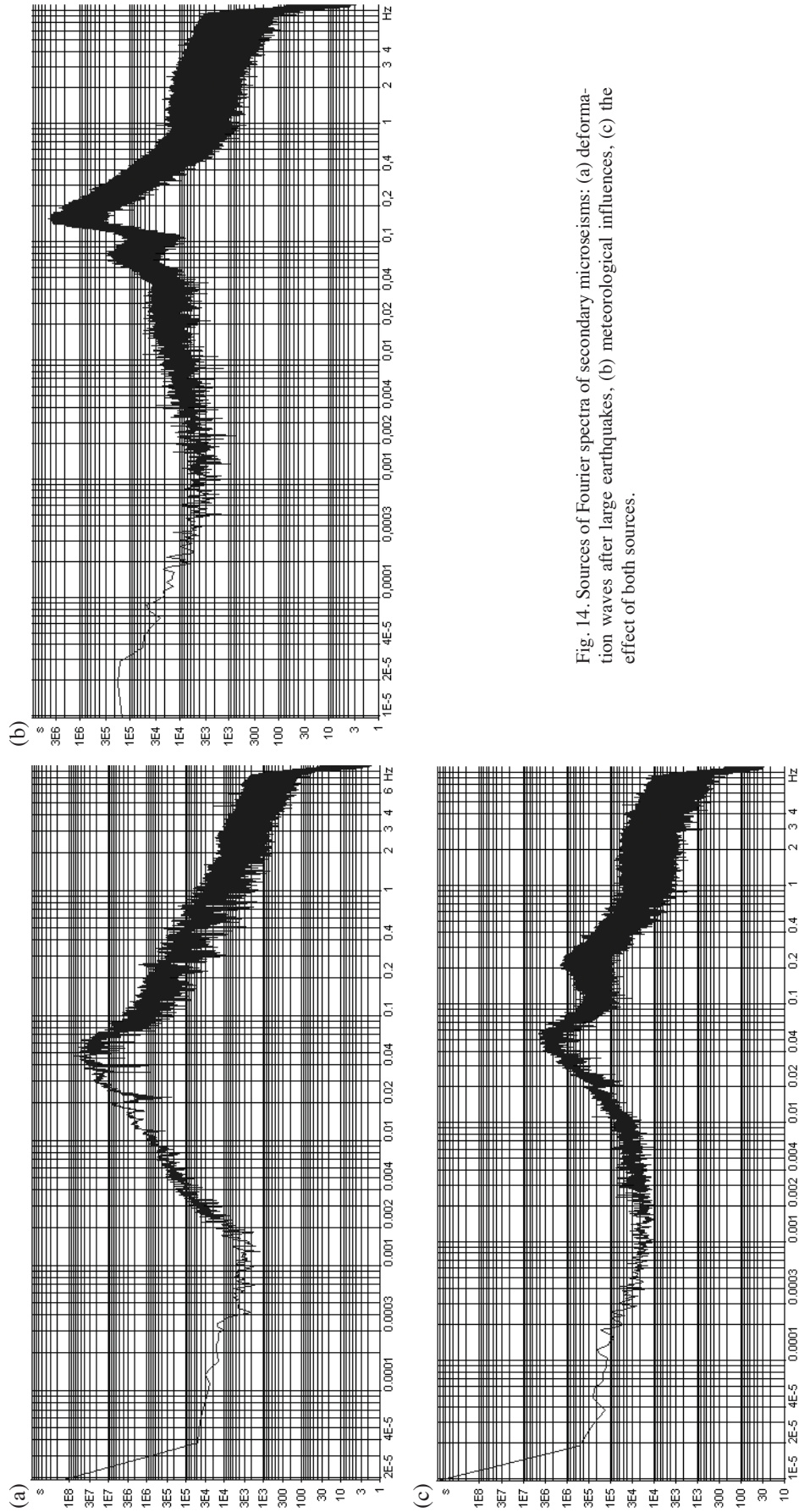
Fig. 14. Sources of Fourier spectra of secondary microseisms: (a) deformation waves after large earthquakes, (b) meteorological influences, (c) the effect of both sources.

thermoelastic waves in the rock mass. This mechanism generates the annual variations of the stress field, which is in the background (frame) for the annual drift of microseisms independent on the storms in the North Atlantic Ocean. The other mechanisms, (1) and (3), are complementary mechanisms to (2). The largest microseism is observed at the time when both (1) and (3) are working together in winter. We can see air pressure variations (storms above the North Atlantic) observed within the time interval of our interest can explain 80% of the anomalous secondary microseisms. The large earthquakes can explain 29% and both mechanisms together can explain 17%, which means that only 8% of anomalously excited secondary microseisms can be generated by another mechanism (see Table. 2).

Generally, it can be concluded that stress state in a rock mass and particular synoptic conditions is a pressumption for microseism excitation. As follows from the result of the complex statistical analysis, no any suitable synoptic situation excites microseisms and vice versa; in effect, if this synoptic situation does not occur, then higher amplitudes of microseisms will not be observed. In particular, the annual drift of microseisms is a symptom which shows that a synoptic situation as such is not a sufficient assumption for the excitation of microseisms. There are a meaningful number of situations where reasonable synoptic situations for excitation of microseisms were introduced, and vice versa.

By analyzing microseism records we found that microseisms have an annual drift similar with temperature, air density and humidity. It is generally known that the response of microseisms to external influences is non-linear. Therefore, in the wintertime, when the stress in rocks is approaching the strength limit of less compact parts of the rock mass, the responses of massif on external forces (i.e., air pressure variations, temperature fluctuations or maximum of microseisms occur when there are extensive barometric lows above northern areas thermoelastic deformation waves) generate large microseisms anomalies.

Microseisms at the OKC seismic station are very sensitive to synoptic situations. The maximum of microseisms occur when there are extensive barometric lows above northern areas, including the North Atlantic area, Iceland, Greenland or Scandinavia, and, when simultaneously, Central Europe is under the influence of an anticyclone (high-pressure area).

REFERENCES

Arctowski, H., 1914: The annual variation of atmospheric pressure in the United States. *Bull. Am. Geogr. Soc.*, **46**, 265-281.

Brimich, L., 2006: Strain measurements at the Vyhne tidal station. *Contrib. Geophys. Geodes.*, **36**, 361-371.

Bromirski, P. D., 2001: Vibrations from the "Perfect Storm". *Geochem. Geophys. Geosyst.*, **2**, doi: 10.1029/2000GC000119. [Link]

Bromirski, P. D. and F. K. Duennebier, 2002: The near-coastal microseism spectrum: Spatial and temporal wave climate relationships. *J. Geophys. Res.*, **107**, doi: 10.1029/2001JB000265. [Link]

Bromirski, P. D., F. K. Duennebier, and R. A. Stephen, 2005: Mid-ocean microseisms. *Geochem. Geophys. Geosyst.*, **6**, Q04009, doi: 10.1029/2004GC000768. [Link]

Cessaro, R. K., 1994: Sources of primary and secondary microseisms. *Bull. Seismol. Soc. Am.*, **84**, 142-148.

Chlumec, 2012: Meteorological data from observatory Chlumec nad Cidlinou. Available at http://www.qpro.cz.

Crespi, M., M. Cuffaro, C. Doglioni, F. Giannone, and F. Riguzzi, 2007: Space geodesy validation of the global lithospheric flow. *Geophys. J. Int.*, **168**, 491-506, doi: 10.1111/j.1365-246X.2006.03226.x. [Link]

Darbyshire, J., 1990: Analysis of twenty microseism storms during the winter of 1987-1988 and comparison with wave hindcasts. *Phys. Earth Planet. Inter.*, **63**, 181-195, doi: 10.1016/0031-9201(90)90017-r. [Link]

Essen, H. H., F. Krüger, T. Dahm, and I. Grevemeyer, 2003: On the generation of secondary microseisms observed in northern and Central Europe. *J. Geophys. Res.*, **108**, doi: 10.1029/2002JB002338. [Link]

Freemeteo, 2007 - 2013: Meteorological data. Available at http://www.freemeteo.com.

Gerstoft, P. and T. Tanimoto, 2007: A year of microseisms in southern California. *Geophys. Res. Lett.*, **34**, L20304, doi: 10.1029/2007GL031091. [Link]

Golovachev, S., M. Dubrov, and V. Volkov, 2011: The interaction between the tropical cyclogenesis and seismic activity as derived from spacecraft and grand-based measuring system. *Present problems of remote sounding of the Earth from cosmos*, **8**, 232-238. (in Russian)

Grob, M., A. Maggi, and E. Stutzmann, 2011: Observations of the seasonality of the Antarctic microseismic signal, and its association to sea ice variability. *Geophys. Res. Lett.*, **38**, L11302, doi: 10.1029/2011GL047525. [Link]

Haubrich, R. A. and K. McCamy, 1969: Microseisms: Coastal and pelagic sources. *Rev. Geophys.*, **7**, 539-571, doi: 10.1029/RG007i003p00539. [Link]

Holub, K., J. Rušajová, and M. Sandev, 2008: The January 2007 windstorm and its impact on microseisms observed in the Czech Republic. *Meteorol. Z.*, **17**, 47-53, doi: 10.1127/0941-2948/2008/0264. [Link]

Holub, K., J. Rušajová, and M. Sandev, 2009: A comparison of the features of windstorms Kyrill and Emma

based on seismological and meteorological observations. *Meteorol. Z.*, **18**, 607-614, doi: 10.1127/0941-2948/2009/0409. [Link]

Hvoždara, M. and L. Brimich, 1988: Thermo-elastic deformations due to the annual temperature variation at the tidal station in Vyhne. *Stud. Geophys. Geod.*, **32**, 129-135, doi: 10.1007/BF01637575. [Link]

Kalenda, P. and L. Neumann, 2010: Static vertical pendulum - observations of anomalous tilt before earthquakes (case study). In: Xie, F. (Ed.), Rock Stress and Earthquakes, 795-803.

Kalenda, P., L. Neumann, and I. Wandrol, 2009: Indirect stress measurement by static vertical pendulum. Proc. of 47th Int. Sci. Conf. Experiment. Analysis of Stress, TU Liberec, 120-128.

Kalenda, P., K. Holub, J. Rušajová, and L. Neumann, 2011: Tracing of travelling of stress-deformation waves after Honshu earthquake. General Assembly of IUGG, IAS-PEI Melbourne, poster.

Kalenda, P., L. Neumann, J. Málek, L. Skalský, V. Procházka, L. Ostřihanský, T. Kopf, and I. Wandrol, 2012: Tilts, Global Tectonics and Earthquake Prediction, SWB, London, 247 pp.

Kalenda, P., K. Holub, J. Rušajová, and L. Neumann, 2013: Microseisms and spreading deformation waves around the globe. NCGT, 1, No. 1, March 2013, 38-57.

Koper, K. D., K. Seats, and H. Benz, 2010: On the composition of Earth's short-period seismic noise field. *Bull. Seismol. Soc. Am.*, **100**, 606-617, doi: 10.1785/0120090120. [Link]

Kurrle, D. and R. Widmer-Schnidrig, 2006: Spatiotemporal features of the Earth's background oscillations observed in central Europe. *Geophys. Res. Lett.*, **33**, L24304, doi: 10.1029/2006GL028429. [Link]

Longuet-Higgins, M. S., 1950: A theory of the origin of microseisms. *Phil. Trans. Roy. Soc. Lond. Math. Phys. Sci.*, **243**, 1-35.

Mareš, S., J. Gruntorád, S. Hrách, M. Karous, F. Marek, M. Matolín, and J. Skopec, 1990: Intrroduction to Applied Geophysics, SNTL, Praha, 677 pp. (in Czech)

Peters, R. D., 2005: Earth oscillations induced by hurricane Katrina. Available at http://serc.carleton.edu/files/eal-abs/hurricanes/2005_Katrina_data.xls.

Rhie, J. and B. Romanowicz, 2006: A study of the relation between ocean storms and the Earth's hum. *Geochem. Geophys. Geosyst.*, **7**, Q10004, doi: 10.1029/2006GC001274. [Link]

Stehly, L., M. Campillo, and N. M. Shapiro, 2006: A study of the seismic noise from its long-range correlation properties. *J. Geophys. Res.*, **111**, B10306, doi: 10.1029/2005JB004237. [Link]

Tanimoto, T., 2007a: Excitation of normal modes by nonlinear interaction of ocean waves. *Geophys. J. Int.*, **168**, 571-582, doi: 10.1111/j.1365-246X.2006.03240.x. [Link]

Tanimoto, T., 2007b: Excitation of microseisms. *Geophys. Res. Lett.*, **34**, L05308, doi: 10.1029/2006GL029046. [Link]

Weatheronline, 1999 - 2013: Meteorological data. Available at http://www.weatheronline.cz/weather/maps/forecastmaps?LANG=cz&CONT=eurok&R=150.

Webb, S. C., 2007: The Earth's 'hum' is driven by ocean waves over the continental shelves. *Nature*, **445**, 754-756, doi: 10.1038/nature05536. [Link]

Wetterzentrale, 1995 - 2013: Synoptic maps. Available at http://www.wetterzentrale.de/topkarten/tkfaxbraar.htm.

Zátopek, A., 1964: Long-period microseisms generated in eastern part of atlantic frontal zone. *Stud. Geophys. Geod.*, **8**, 127-139, doi: 10.1007/BF02607177. [Link]

Zátopek, A., 1975: On the long-term microseismic activity and some related results. *Stud. Geophys. Geod.*, **19**, 14-24, doi: 10.1007/BF01626474. [Link]